Dynamic simulation and control of sit-to-stand motion

Sébastien Barthélemy, Camille Salaün, Philippe Bidaud

Laboratoire de Robotique de Paris

Université Paris 6 / CNRS

18, route du Panorama

92265 Fontenay Aux Roses - France

email: barthelemy@robot.jussieu.fr, salaun@robot.jussieu.fr, bidaud@robot.jussieu.fr

Abstract— **This paper investigates the strategies used during the human sit to stand movement. The analysis was carried out by means of the 3D videographic examination methods and a posturographic platform. The joint trajectories corresponding to the motion were reconstructed using the Humanoid Motion Analysis and Simulation (HuMAnS) toolbox developed at INRIA-Grenoble. The reliability of the dynamic model used in simulation was analysed by comparing the inertial forces computed from the reconstructed motion with the recorded ground reaction forces.**

I. INTRODUCTION

In humanoid robot the number of available degrees of freedom (dofs) of the whole body is generally greater than needed for any particular task. Such redundancy affords flexible and adaptable motor behaviors and may be used to optimize the motion. Potential solutions for optimal coordination strategies can be inspired by human motor behaviors.

Several human motor control schemes had been suggested, such as simple servo-loop [?] [?], combination of feedforward and feedback control [?] [?] or optimal control [?]. The sensorimotor intrinsic latencies and some experiments [?] seem to exclude a "feedback-only"control scheme. Thus, it is likely that the central nervous system constructs an internal model that encapsulates the dynamic task and use it (by inverting it) to compute the control vector corresponding to the "desired trajectory".

The role of the feedback part of this control scheme is to compensate for perturbations, to nullify the static error and to provide data to update the internal model.

The feedforward control relies on an accurate internal representation of stability limits, which must be a function of natural dynamics of the musculoskeletal system as well as environmental and intrinsic constraints (e.g, minimum energy, feasable joint accelerations, . . .). Constraints may be imposed as the result of the optimization of some mechanical cost function associated with the production of movement to produce motor synergies which tend to maximize the performances of the motor act. Such movement coordination patterns can be observed in many complex activities such as pointing, reaching, locomotion, etc . . .

This trajectory pattern can indeed vary with repetitions, intentional modifications of the referent pattern, task constraints and history-dependent changes in the neuromuscular system.
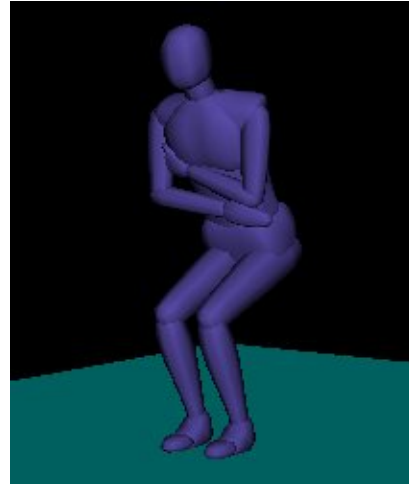

Fig. 1. A graphic output from the HuMAnS toolbox, showing the reconstructed StS movement.

The aim of this work is to extract knowledge regarding the execution of a specific motor task.

It considers more specifically the motion coordination pattern of the sit-to-stand movement. Rising from a sitting position is one of the most difficult and mechanically demanding functional operations facing a human beings. A deeper understanding of how the biomechanics of this movement is linked to control strategies of the postural system can help in approaching other questions such as for the synthesis perceptuo-motor primitives for humanoid imitation as well as for the design of assistive dynamic stander devices.

A motion capture system was used to measure the movements of several sit-to-stand motions. Simultaneously, the ground reaction force was recorded with a posturographic force platform. The joint trajectories corresponding to the motion were reconstructed using the Humanoid Motion Analysis and Simulation (HuMAnS) toolbox developed at INRIA-Grenoble. The reliability of the dynamic model used in simulation was analysed by comparing the inertial forces computed from the reconstructed motion with the recorded ground reaction forces.

II. Experimental results

A. Experimental protocol

Experimental data of few StS motions were recorded at the laboratory of "Adaptation Perceptivo-Motrice et Apprentissage" (LAPMA, UPRES EA 3691).

The subjects started sitting on a 45 centimeters chair in a static comfortable position, crossing their arms on their chest. The only contacts were beetween the buttock-thigh and the seat and the feet on the ground. The subjects were asked to stand up in a "normal way", ie. at self chosen speed, without moving their feet. Several measurements were realised from which we present here only a representative one from 26 years old man weighting 92 kg and measuring 1.93m.

Data were extracted from two different sources : a motion capture system from Vicon [?] and a posturographic force platform. The force and motion data were synchronized by the Vicon system.

The Vicon system measured the cartesian positions of optical markers glued on the subject at anatomical landmarks at a sampling frequency of 100 Hz. The samples were then filtered with a sixth order low-pass Butterworth filter whose cut-off frequency was set to 5 Hz.

The posturographic force platform (Model BP-9001800, AMTI, Watertown, USA) was placed under the subject and the chair, as shown figure 2, in order to measure all the reaction forces. It's sampling frequency was 100 Hz.

Fig. 2. The experimental setup, with the force platform measuring both chair and ground reaction forces.

B. Relation between measured forces and motion

Let's consider the general case of the subject sitting on the chair with its feet on the ground. In a galilean frame, the dynamic equilibrium of wrenches acting on its body can be written (at any point $\mathbf{Q}$) as:

$$\mathbf{W}^Q_{\text{i}\to\text{sbj}} = \mathbf{W}^Q_{\text{gr}\to\text{sbj}} + \mathbf{W}^Q_{\text{gd}\to\text{sbj}} + \mathbf{W}^Q_{\text{ch}\to\text{sbj}} \quad (1)$$

where $\mathbf{W}^Q_{\text{i}\to\text{sbj}}$ and $\mathbf{W}^Q_{\text{gr}\to\text{sbj}}$ are respectively inertial and gravitational resultant wrenches acting on the subject. Their resultant force ($\mathbf{R}$) and moment ($\mathbf{M}^Q$) could be written as:

$$\mathbf{R}_{\text{gr}\to\text{sbj}} = m_{\text{sbj}}\mathbf{g}$$
$$\mathbf{M}^Q_{\text{gr}\to\text{sbj}} = m_{\text{sbj}}\mathbf{Q}\mathbf{G}_{\text{sbj}} \times \mathbf{g}$$
$$\mathbf{R}_{\text{i}\to\text{sbj}} = m_{\text{sbj}}\ddot{\mathbf{O}\mathbf{G}}_{\text{sbj}}$$
$$\mathbf{M}^Q_{\text{i}\to\text{sbj}} = \left(m_{\text{sbj}}\mathbf{Q}\mathbf{G}_{\text{sbj}} \times \ddot{\mathbf{O}\mathbf{G}}_{\text{sbj}} + \dot{\mathbf{H}}_{\text{sbj}}\right)$$

with m_{sbj} the subject's mass, $\mathbf{G}_{\text{sbj}}$ its center of mass, $\mathbf{g}$ the acceleration of gravity and $\mathbf{O}$ the origin of the galilean frame.
$\mathbf{W}^Q_{\text{gd}\to\text{sbj}}$ and $\mathbf{W}^Q_{\text{ch}\to\text{sbj}}$ are respectively the wrenches of ground and chair contact forces on the subject.

Let's now apply the Newton-Euler equation on the system composed by the subject and the chair and then to the chair alone.

$$\mathbf{W}^Q_{\text{i}\to\{\text{sbj+ch}\}} = \mathbf{W}^Q_{\text{gr}\to\{\text{sbj+ch}\}} + \mathbf{W}^Q_{\text{gd}\to\{\text{sbj+ch}\}}$$
$$\mathbf{W}^Q_{\text{i}\to\text{ch}} = \mathbf{W}^Q_{\text{gr}\to\text{ch}} + \mathbf{W}^Q_{\text{gd}\to\text{ch}} - \mathbf{W}^Q_{\text{ch}\to\text{sbj}}$$

Since the chair doesn't move these wrenches can be written :

$$\mathbf{W}^Q_{\text{i}\to\{\text{sbj+ch}\}} = \mathbf{W}^Q_{\text{i}\to\text{sbj}}$$
$$\mathbf{W}^Q_{\text{gd}\to\{\text{sbj+ch}\}} = \mathbf{W}^Q_{\text{gd}\to\text{sbj}} + \mathbf{W}^Q_{\text{gd}\to\text{ch}}$$
$$= \mathbf{W}^Q_{\text{gd}\to\text{sbj}} + \mathbf{W}^Q_{\text{ch}\to\text{sbj}} - \mathbf{W}^Q_{\text{gr}\to\text{ch}}$$

Since the posturographic force platform offset was adjusted to be zero with the chair on it, the wrench it measured, $\mathbf{W}^Q_{\text{meas}}$, is :

$$\mathbf{W}^Q_{\text{meas}} = \mathbf{W}^Q_{\text{gd}\to\text{sbj}} + \mathbf{W}^Q_{\text{ch}\to\text{sbj}}$$
$$= \mathbf{W}^Q_{\text{i}\to\text{sbj}} - \mathbf{W}^Q_{\text{gr}\to\text{sbj}}$$

Hence, the force measured by the platform can be directly compared to the gravity and inertia forces computed from the subject's inertial model and the derivatives of the reconstructed joint trajectories.

C. Human model and motion reconstruction

In order to reconstruct the motion and to perform simulations, we used the Humanoid Motion Analysis and Simulation (HuMAnS) toolbox developed by the BIPOP team at INRIA-Grenoble ([?],[?]). This GPL licensed software provides a biomechanical model of a complete human body together with a simulation engine handling rigid contacts between the model and the environment.

The human model has 36 actuated dofs corresponding to 16 joints (6 dofs per leg, 8 dofs per arm, 2 dofs for each sterno-clavicular articulation, 3 dofs for the thorax and 3 dofs for the head). The model is "free flying", meaning that no part of the body is assumed to remain fixed in space. Six additional parameters, or "virtual dofs" are therefore required for positioning the body in space (the 6 virtual dofs are illustrated fig. 3). The model mass, height and limb lengths can be parametrised to cope with the subject ones. The model inertia and anatomical landmarks positions are then computed from these settings, according to biomechanical sources ([?], [?]).

Using the anatomical landmarks positions and jacobians provided by the HuMAnS toolbox, we reconstructed the joints trajectories by minimizing the quadratic error between the landmarks on the model and the measured ones.

In order to check the validity of a reduced 3-R model of the motion in the sagittal plane, we performed this reconstruction two times. The first time, we let the reconstruction algorithm use every joint (36 dofs), while the second time, only the ankle, knee and hip flexion-extension rotations (3 dofs) were available to the reconstruction procedure, and the feet were constrained to remain on the ground. The restricted model used for the second reconstruction can be seen figure 3. The joints of both legs were constrained to remain equal.
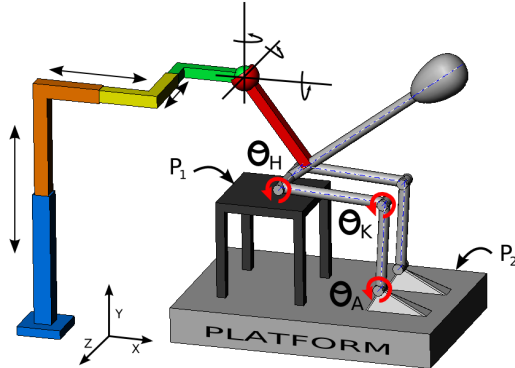

Fig. 3.   Kinematic model used for the second reconstruction.

The resulting joint trajectories were then filtered with a sixth order Butterworth's filter (cut-off frequency : 5 Hz) and finally differentiated to obtain the joint velocities and accelerations.

The dynamical model is written in HuMAnS with generalized coordinates :

$$\mathbf{M}(\mathbf{q})\ddot{\mathbf{q}} + \mathbf{N}(\mathbf{q}, \dot{\mathbf{q}}) = \mathbf{G}(\mathbf{q}) + \mathbf{\Gamma}(t) + \mathbf{J}_c^T \lambda \qquad (2)$$

where $\mathbf{M}(\mathbf{q})$, $\mathbf{N}(\mathbf{q}, \dot{\mathbf{q}})$ and $\mathbf{G}(\mathbf{q})$ are respectively the inertia matrix, the vector of Coriolis and centrifugal effects and the vector of gravity effects. $\mathbf{\Gamma}(t)$ is the vector of generalized torques and $\mathbf{J}_c^T \lambda$ is the torques generated by contact forces.

The model can be decomposed between actuated and non-actuated (virtual) dofs $\mathbf{q} = \begin{pmatrix} \mathbf{q}_a \\ \mathbf{q}_v \end{pmatrix}$ and the equation (2)

rewritten as follow illustrates again that inertial and gravity on the virtual links can only be compensated for by the contact forces.

$$\mathbf{M}_a(\mathbf{q})\ddot{\mathbf{q}} + \mathbf{N}_a(\mathbf{q}, \dot{\mathbf{q}}) = \mathbf{G}_a(\mathbf{q}) + \mathbf{\Gamma}_a(t) + \mathbf{J}_{ca}^T \lambda \qquad (3)$$
$$\mathbf{M}_v(\mathbf{q})\ddot{\mathbf{q}} + \mathbf{N}_v(\mathbf{q}, \dot{\mathbf{q}}) = \mathbf{G}_v(\mathbf{q}) + \mathbf{0} + \mathbf{J}_{cv}^T \lambda \qquad (4)$$

Knowing $\mathbf{q}$, $\dot{\mathbf{q}}$ and $\ddot{\mathbf{q}}$ from the motion reconstruction, we can compute $(\mathbf{M}_v(\mathbf{q})\ddot{\mathbf{q}} + \mathbf{N}_v(\mathbf{q}, \dot{\mathbf{q}}) - \mathbf{G}_v(\mathbf{q}))$ (or, equivalently, $\left(\mathbf{W}_{i \to sbj}^Q - \mathbf{W}_{gr \to sbj}^Q \right)$) and compare it with the measured ground reaction forces. As seen figure 4, the reconstructed forces are very similar to the recorded ones for both the 36-dofs and 3-dofs reconstructions, while the correspondance of the reconstructed moment is less impressive, suggesting some discrepencies between the model inertias and the real ones.
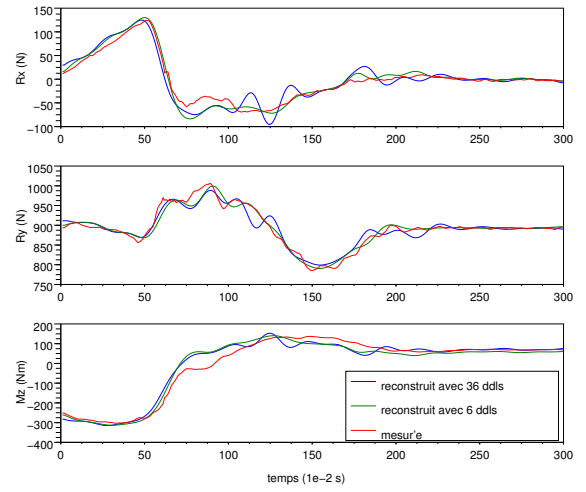

Fig. 4.   Ground reaction forces measured by the force platform and computed from the reconstructed motion with all the (36) dofs and the with only 3 dofs (planar 3-R model).$\mathbf{R}_{meas,x}$ is the force along the antero-posterior direction, $\mathbf{R}_{meas,y}$ is the force along the vertical direction and $\mathbf{M}_{meas}^O$ is the moment computed at the ankle projection on the ground

The small differences which can be observed between the 3-dofs reconstructions and the force platform data show that a planar 3-R model is a good approximation of the recorded motion.

D. Motion analysis

The reconstructed motion and the model provided by the HuMAnS toolbox (either with all dofs controlled or not) can be used to compute difficultly measurable physical values, such as the angular momentum at the center of masses (CoM). As shown figure 5, the angular momentum varies highly during StS movement, in contrast with measurements realised on humans walking where it seems to be regulated ([?]).

This phenomenon can be understood qualitatively : the Euler law of motion states that whitout external intervention, the angular momentum is constant. After the take-off, the body is submitted to the action of the gravity and of the ground reaction on its feet. As the center of pressure of the
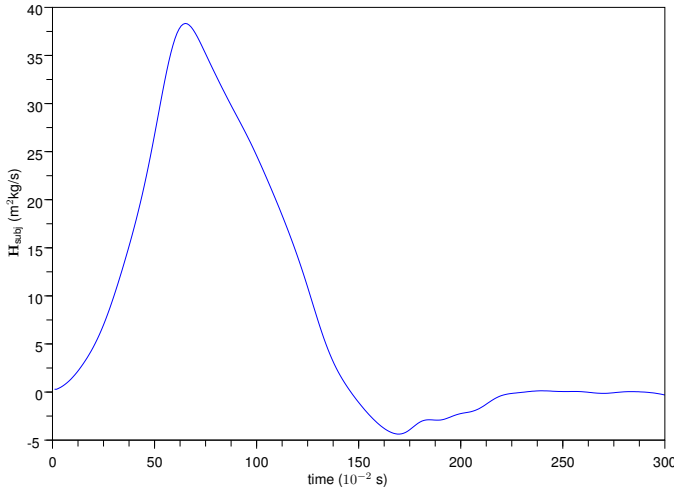
Fig. 5. Angular momentum computed at the CoM

contact force lies in the base of support (BoS), as long as the CoM is not over the BoS, the effect of the gravity is decreases the angular momentum at CoM. The only way to stand up (fastly) is thus to accumulate enough angular momentum *before* lift-off to avoid falling down backward due to gravity *after* lift-off.

Among other physical values of interest is the zero moment point (ZMP) also called center of pressure (CoP). This points is only defined (in its original form) if all the contact with the studies body lie in the same plane. Therefore, during StS movement, the ZMP is only defined after the lift-off.

The ZMP is defined as the only point on the contact plane (the ground, noted $\mathcal{P}_1$) where the moment of the gravity and inertial wrenches is perpendiculary to the contact surface. Thus, with $\mathbf{n}$ the unit normal to $\mathcal{P}_1$ the point is defined as

$$\mathbf{Z} \in \mathcal{P}_1 / \left(\mathbf{M}^Z_{i\to sbj} - \mathbf{M}^Z_{gr\to sbj}\right) \times \mathbf{n} = \mathbf{0}$$

and may be computed as

$$\mathbf{OZ} = \frac{\left(\mathbf{M}^O_{i\to sbj} - \mathbf{M}^O_{gr\to sbj}\right) \times \mathbf{n}}{\left(\mathbf{R}_{i\to sbj} - \mathbf{R}_{gr\to sbj}\right) \cdot \mathbf{n}}$$

where $\mathbf{O}$ is any point where the moments of gravity or inertia are known (the HuMAnS origine for instance).

After lift-off, $\mathbf{W}^Q_{ch\to sbj} = \mathbf{0}$ at any point $\mathbf{Q}$, thus from eq. (1) it is straightforward that

$$\mathbf{M}^Z_{gd\to sbj} \times \mathbf{n} = \mathbf{0}$$

However, when considered from the point of view of contact forces, the point is preferably called the CoP, because this is also the point where the moment of the pressure forces (the component of contact forces normal to $\mathcal{P}_1$) vanish. One can explicit the CoP using surfacic contact force at every point $\mathbf{A}$ of the contact surface S:

$$\mathbf{OP} = \frac{\mathbf{n} \times \mathbf{M}^O_{gd\to sbj}}{\mathbf{R}_{gd\to sbj} \cdot \mathbf{n}}$$

$$= \frac{\mathbf{n} \times \left(\int_{A\in S} \mathbf{OA} \times \mathbf{f}_{gd\to sbj(A)} dS\right)}{\left(\int_{A\in S} \mathbf{f}_{gd\to sbj(A)} dS\right) \cdot \mathbf{n}}$$

$$= \frac{\int_{A\in S} \mathbf{OA} \cdot \mathbf{n} \cdot \mathbf{f}_{gd\to sbj(A)} dS}{\int_{A\in S} \mathbf{n} \cdot \mathbf{f}_{gd\to sbj(A)} dS}$$

As the pressure force are always positive ($\forall A \in S : \mathbf{n} \cdot \mathbf{f}_{gd\to sbj(A)}$), the CoP (and the ZMP, as they are the same points) are lie in the convex hull of the contact points, called the base of support.

The ZMP is widely used among walking robots to check if a desired motion is feasible or not, by checking whether or not it leads to a ZMP inside the BoS. However, if the contacts do not lie in the same plane, like during the first part of the StS motion, the ZMP is useless. Some extended definitions of the ZMP, such as the Generalized ZMP and the Foot Rotation Indicator (FRI) may be usefull in such cases, however, we prefer to use a more general way of handling contact-related constraints, as will be explained in section III-B.

III. COMMAND

The aim of this control scheme is to rise a humanoid from a seated position. To properly control the motion, the control law has to handle the contacts in order to (1) use them to control the global body position and (2) avoid trying to perform unfeasable motions. We present here a control scheme that permit to handle multiple tasks and contraints and a control law (or task specification) that reproduces the StS motion.

A. Control scheme

Park already proposed such a framework [**?**] using operational space and dynamically consistant pseudoinverse. We propose here to formulate a similar strategy as an quadratic minimisation under linear constraint problem, in order to take the contacts constraints directly into account.

Let's consider two desired motions in task space $\ddot{\mathbf{x}}_{1d}$ and $\ddot{\mathbf{x}}_{2d}$. Knowing their jacobian (and their first derivative) one can link these motions to the joint acceleration $\ddot{\mathbf{q}}$:

$$\dot{\mathbf{x}}_1 = \mathbf{J}_1\dot{\mathbf{q}} \qquad \ddot{\mathbf{x}}_1 = \mathbf{J}_1\ddot{\mathbf{q}} + \dot{\mathbf{J}}_1\dot{\mathbf{q}}$$
$$\dot{\mathbf{x}}_2 = \mathbf{J}_2\dot{\mathbf{q}} \qquad \ddot{\mathbf{x}}_2 = \mathbf{J}_2\ddot{\mathbf{q}} + \dot{\mathbf{J}}_2\dot{\mathbf{q}}$$

The point will be to find the proper generalized motion $\ddot{\mathbf{q}}$ that minimises the norm between the desired motions while respecting the constraints. We chose the acceleration energy $||\ddot{\mathbf{x}}_{1d} - \ddot{\mathbf{x}}_d||_{\mathbf{\Lambda}_1}$ as the norm in order to use a physically consistant and invariant criteria, using the inertia matrix in the task space :

$$\mathbf{\Lambda}_i = \left(\mathbf{J}_i\mathbf{M}^{-1}\mathbf{J}_i^{\mathbf{T}}\right)^{\dagger} \qquad i \in \{1, 2\} \qquad (5)$$

Usually the $\left(\mathbf{J_i M^{-1} J_i^T}\right)$ matrices are of full rank and there is no need to use a pseudoinverse. However, when the task jacobian becomes singular (when $\mathbf{J_i}$ rank drops), we should use singular value decomposition to compute $\mathbf{\Lambda_i}$ in order to avoid any bad behaviour of the control scheme.

Now, minimizing the quantity

$$||\ddot{\mathbf{x}}_{\mathrm{id}} - \ddot{\mathbf{x}}_{\mathrm{i}}||_{\mathbf{\Lambda_i}} = \left(\ddot{\mathbf{x}}_{\mathrm{id}} - \ddot{\mathbf{x}}_{\mathrm{i}}\right)^T \mathbf{\Lambda_i} \left(\ddot{\mathbf{x}}_{\mathrm{id}} - \ddot{\mathbf{x}}_{\mathrm{i}}\right)$$

is equivalent to minimize

$$\frac{1}{2}\,\ddot{\mathbf{q}}^T \mathbf{Q_i}\ddot{\mathbf{q}}\;\; + \ddot{\mathbf{q}}^T \mathbf{p_i}$$
$$\mathbf{Q_i} = \left(\mathbf{J_i}^T \mathbf{\Lambda_i J_i}\right)$$
$$\mathbf{p_i} = -\mathbf{J_i}^T \left(\ddot{\mathbf{x}}_{\mathrm{i}} - \dot{\mathbf{J}}_{\mathrm{i}}\dot{\mathbf{q}}\right)$$

At this stage, we can formulate the minimization problem as :

$$\frac{1}{2}\,\ddot{\mathbf{q}}^T \left(\mathbf{Q_1 + Q_2}\right)\ddot{\mathbf{q}}\;\; + \ddot{\mathbf{q}}^T \left(\mathbf{p_1 + p_2}\right) \qquad (6)$$

If the two tasks are incompatible, the control law will look for a trade off between them. This is knowns as the "ponderation strategy".

In order to prevent the second task to interfere with the first, we also introduce hierarchisation between the tasks by projecting any joint acceleration on the first task kernel before the energy associated to the second task. If $\mathbf{P_1}$ is a projector on the first task kernel, the hierarchised version can simply be written as follow:

$$\frac{1}{2}\,\ddot{\mathbf{q}}^T \left(\mathbf{Q_1 + Q_{21}}\right)\ddot{\mathbf{q}}\;\; + \ddot{\mathbf{q}}^T \left(\mathbf{p_1 + p_{21}}\right) \qquad (7)$$
$$\mathbf{Q_{21}} = \left(\mathbf{P_1}^T \mathbf{Q_2 P_1}\right)$$
$$\mathbf{p_{21}} = \mathbf{P_1}^T \mathbf{p_2}$$

For the minimization problems stated in equations (6) and (8) to have a unique solution, their hessian matrix must be of full rank. While humanoid robots are highly redundant, this is often not the case. One should therefore add another criterium to minimize, projected on the other task nullspaces (what Khatib and Sentis call the "posture subspace"). A pertinent criterium is the acceleration energy $\frac{1}{2}\ddot{\mathbf{q}}^T \mathbf{M}\ddot{\mathbf{q}}$, but many others may be used. Therefore equation (8) is rewritten :

$$\frac{1}{2}\,\ddot{\mathbf{q}}^T \left(\mathbf{Q_1 + Q_{21} + Q_{321}}\right)\ddot{\mathbf{q}}\;\; + \ddot{\mathbf{q}}^T \left(\mathbf{p_1 + p_{21}}\right) \quad (8)$$
$$\mathbf{Q_{321}} = \left(\left(\mathbf{P_1 P_2}\right)^T \mathbf{M}\left(\mathbf{P_1 P_2}\right)\right)$$

Minimizing this criteria is exactly equivalent to using the dynamically consistent pseudoinverse (cf. [**?**], [**?**]). However, as we will show in next section, this formulation allows to account for inequality constraints and to use directly quadratic programming libraries such as qld.

the $\mathbf{\Lambda_i}$ matrices from eq. (5) and the kernel space projectors $\mathbf{P_i}$ are computed using singular value decomposition of $\left(\mathbf{J_i M^{-1} J_i^T}\right)$, insuring good behaviour of the control scheme when the task jacobian is singular.

B. Constraints

As pointed out by Wieber and others ([**?**], [**?**]), with the equation (1) (or equivalently eq. (4)), the constraints existing on contact forces are reported on the robot motion. In other words, if we intend to perform a desired motion $\ddot{\mathbf{q}}_{\mathrm{des}}$, we have to check if there exist contact forces λ respecting the Coulomb and Signorini laws and subject to equation (4). The equation (3) is not considered because, under the assumption of perfect actuators, one can always find generalized torques $\mathbf{\Gamma_a}$ satisfying both eq. (3) with $\ddot{\mathbf{q}} = \ddot{\mathbf{q}}_{\mathrm{des}}$ and contact conditions.

For the j^{est} ponctual contact, knowing the contact unit normal $\mathbf{n_j}$ and the jacobian of the contact point $\mathbf{J_{cj}}$, one can write the Signorini law as

$$\mathbf{n_j} \cdot \lambda_j \geq 0 \qquad (9)$$

Coulomb's friction cone can also be linearized using several unit vectors $\mathbf{t_{j1}, t_{j2}, \ldots}$ in the tangential plane, leading to the constraints :

$$\mathbf{t_{j1}} \cdot \lambda_j \leq k\mu_s\,\mathbf{n_j}\cdot\lambda_j$$
$$-\mathbf{t_{j1}} \cdot \lambda_j \leq k\mu_s\,\mathbf{n_j}\cdot\lambda_j$$
$$\mathbf{t_{j2}} \cdot \lambda_j \leq k\mu_s\,\mathbf{n_j}\cdot\lambda_j$$
$$-\mathbf{t_{j2}} \cdot \lambda_j \leq k\mu_s\,\mathbf{n_j}\cdot\lambda_j$$
$$...$$

These equations can be concatenated to a more compact matrix form

$$\mathbf{A}\lambda \leq \mathbf{b} \qquad (10)$$

Now, from eq. (4), if J_c is inversible, we can link the forces λ to the accelerations using the contact space inertia matrix ([**?**])

$$\mathbf{\Lambda_c} = \left(\mathbf{J_c M^{-1} J_c^T}\right)^{-1} \qquad (11)$$

and eq. (10) can now be rewritten :

$$\mathbf{A \Lambda_c J_c}\left(\ddot{\mathbf{q}} + \mathbf{M^{-1}}\left(\mathbf{N(q,\dot{q}) - G(q)}\right)\right) \leq \mathbf{b} \qquad (12)$$

The equations (12) and (8) define a QP problem.

C. Task space for sit-to-stand motion

We tried the presented control scheme with the planar 3-R model and with a single (non sliding) contact point at the hip, modelling the interaction between the chair and the subject.

The planar 3-R model is very simple, but is sufficient to capture the caracteristics of the motion. The interaction model chosen for the chair effects is more restrictive, but sit-to-stand motion are still possible.

To maintain the model feet on the ground, we added bilateral contraints to eq. (12), preventing the corresponding contact points to move.

Inspired by the considerations on the angular momentum presented earlier in this paper and by the sigmoid shape of the $\mathbf{M}_{\mathrm{meas}}^O$ curve (Fig. 4), we chose as the first task space the CoM rotational acceleration used the (normalized) recorded moments as desired acceleration. The second task space was

the vertical position of the head, in order to enforce the upright posture.

The resulting motion showed two phase more demarked than in the real one, but the hip contact was properly handled: the lift-off occured without any "manual specification".